 doi:10.20944/preprints201912.0023.v1

Article

Polarizability-dependent sorting of microparticles using continuous-flow dielectrophoretic chromatography with a frequency modulation method

Jasper Giesler [1], Georg R. Pesch [1,2,*], Laura Weirauch [1], Marc-Peter Schmidt [3], Jorg Thöming [1,2] and Michael Baune[1]

1 University of Bremen, Chemical Process Engeneering, Leobener Straße 6, 28359 Bremen, Germany
2 University of Bremen, MAPEX Center for Materials and Processes, 28359 Bremen, Germany
3 Brandenburg University of Applied Sciences, Department of Engineering, Magdeburger Straße 50, 14770 Brandenburg an der Havel, Germany
* Correspondence: gpesch@uni-bremen.de

Abstract: The separation of microparticles with respect to different properties such as size and material is a research field of great interest. Dielectrophoresis, a phenomenon which is capable of addressing multiple particle properties at once, can be used to perform a chromatographic separation. However, the selectivity of current dielectrophoretic particle chromatography (DPC) techniques is limited. Here we show a new approach for DPC based on differences in the dielectrophoretic mobilities and the crossover frequencies of polystyrene particles. Both differences are addressed by modulating the frequency of the electric field to generate positive and negative dielectrophoretic movement to achieve multiple trap and release cycles of the particles. A chromatographic separation of different particle sizes revealed a voltage dependency of this method. Additionally, we showed the frequency bandwidth influence on separation using one example. The DPC method developed was tested with model particles but offers possibilities to separate a broad range of plastic and metal microparticles or cells and to overcome currently existing limitations in selectivity.

Keywords: Dielectrophoresis, DEP, microparticles, polystyrene, chromatography, interdigitated electrodes, microfluidic, separation

1. Introduction

Separating microparticles according specific properties such as size, material and shape is a research area of great interest for instance in cell or biomolecule manipulation [1–5] and waste recovery [6,7]. To separate microparticles field flow fractionation [8], gel electrophoresis [9], and size-exclusion chromatography [10] are state-of-the-art approaches. In these processes, however, either selectivity or throughput is limited. Dielectrophoresis, which is referred to as the movement of polarizable particles in an inhomogeneous electric field, offers an alternative tool to address a wide range of particles and at the same time is able to achieve relevant throughputs [11,12]. Additionally, the dielectrophoretic force not only depends on one specific property of a particle, but on a variety of particle properties, such as size [13,14], permittivity and electrical conductivity [1]. For increasing the resolution of dielectrophoretic separation techniques, chromatographic approaches are a promising concept. Since dielectrophoretic particle chromatography was introduced by Washizu *et al.* [5], different approaches were made using selective trapping of particles [15,16], packed bed columns [17] or stepwise change of the frequency [18]. Aldaeus *et al.* [19] developed an analytical model for a dielectrophoretic particle chromatography (DPC) device which is based on multiple trap and release cycles for fractionation. Another technique to manipulate micrometer sized particles is using traveling-wave dielectrophoretic separators [20,21]. In these microfluidic devices, a 90° phase angle is present between adjacent

Preprints (www.preprints.org) | NOT PEER-REVIEWED | Posted: 3 December 2019 doi:10.20944/preprints201912.0023.v1

electrodes, which changes the dielectrophoretic movement a particle experiences [22,23]. Current dielectrophoretic chromatography techniques are limited in selectivity and lacking the applicability for a wide range of particle mixtures, since the separation depends on strongly diverging polarizabilities. Other techniques such as the travelling-wave systems are usually complex to fabricate and operate [21,24].

To overcome these limitations we developed a system that employs the novel concept of frequency-modulated dielectrophoretic particle chromatography. Its frequency changes constantly to allow for separating particles with respect to their dielectrophoretic mobilities. Here, the switching between positive and negative dielectrophoretic movement generates multiple trap and release cycles of microparticles to achieve a chromatographic separation. The simplicity of our approach allows for a simple fabrication and operation and could be easily scaled up by using different ways to introduce the electric field graident (for example using a porous medium as demonstrated in our recent work [11])

2. Method

In classic chromatographic processes (e.g. gas chromatography) mixtures are separated due to different interactions of sample and stationary phase, leading to characteristic retention times for each class in the sample. In dielectrophoretic particle chromatography the stationary phase is represented by the inhomogeneous electric field which rises over interdigitated electrodes. The electrode chip forms the bottom of a microfluidic device, where a polydimethylsiloxane (PDMS) channel is used as separation column. The microparticle suspension is injected into the flow chamber and further transported by a carrier flow. The electrodes are connected to an AC voltage source to generate a highly inhomogeneous electric field. This gives rise to a dielectrophoretic force on the particle caused by the action of the inhomogeneous field on the induced dipole (or multipole) of the particle. The dielectrophoretic force $\mathbf{F}_{\mathrm{DEP}}$ can be expressed as

$$\mathbf{F}_{\mathrm{DEP}} = \pi r_{\mathrm{p}}^3 \varepsilon_{\mathrm{m}} \mathrm{Re}\left(\frac{\tilde{\varepsilon}_{\mathrm{p}} - \tilde{\varepsilon}_{\mathrm{m}}}{\tilde{\varepsilon}_{\mathrm{p}} + 2\tilde{\varepsilon}_{\mathrm{m}}}\right) \nabla |\mathbf{E}|^2, \tag{1}$$

with r_{p} representing the particles radius, $\nabla|\mathbf{E}|^2$ the electric field gradient squared and $\tilde{\varepsilon}_{\mathrm{p}}$ the complex permittivity of the particles and the medium ($\tilde{\varepsilon}_{\mathrm{m}}$), respectively. The velocity due to dielectrophoresis $\mathbf{v}_{\mathrm{DEP}}$ in a stationary fluid can be calculated by dividing the dielectrophoretic force by the friction factor f:

$$\mathbf{v}_{\mathrm{DEP}} = \mu_{\mathrm{DEP}} \nabla |\mathbf{E}|^2 = \frac{\pi r_{\mathrm{p}}^3 \varepsilon_{\mathrm{m}} \mathrm{Re}\left(\frac{\tilde{\varepsilon}_{\mathrm{p}} - \tilde{\varepsilon}_{\mathrm{m}}}{\tilde{\varepsilon}_{\mathrm{p}} + 2\tilde{\varepsilon}_{\mathrm{m}}}\right) \nabla |\mathbf{E}|^2}{f}. \tag{2}$$

Here, μ_{DEP} is the dielectrophoretic mobility, which not only provides the direction of the movement of the microparticles, but incorporates the radius of the particles and fluid properties additionally. The direction of the DEP force can be determined by calculating the real part of the Clausius-Mossotti factor $\mathrm{Re}(CM)$:

$$CM = \frac{\tilde{\varepsilon}_{\mathrm{p}} - \tilde{\varepsilon}_{\mathrm{m}}}{\tilde{\varepsilon}_{\mathrm{p}} + 2\tilde{\varepsilon}_{\mathrm{m}}}. \tag{3}$$

The complex permittivity expands the permittivity ε of a material and incorporates the material's conductivity σ and the angular frequency ω of the electric field:

$$\tilde{\varepsilon} = \varepsilon_0 \varepsilon_{\mathrm{r}} - i\frac{\sigma}{\omega}. \tag{4}$$

 doi:10.20944/preprints201912.0023.v1

For low frequencies, Re(CM) is dominated by the conductivity of the material, as the frequency increases the permittivity becomes more important. The conductivity of small insulating particles (such as the used polystyrene particles) is dominated by their surface conductance K_S [25]:

$$\sigma_p = \frac{2K_S}{r_p}. \tag{5}$$

When particles are less polarizable than the surrounding medium (Re$(CM) < 0$, nDEP), they move against the electric field gradient and towards low field regions. Contrary, more polarizable particles (Re$(CM) > 0$, pDEP) are directed with the gradient towards field maxima. In the current setup field maxima are located close to the edges of the interdigitated electrodes at the bottom and local field minima can be found at the top of the channel. Depending on the polarization, particles are either trapped close to the edges of the electrode (pDEP) or at the top (nDEP). Therefore, the trapping location will be strongly affected by the applied field's frequency due to the frequency-dependence of Re(CM) (Equation 4).

When a particle hits a surface the particle-wall interactions can be strong enough for particles to adhere even in the absence of an externally applied field force (i. e., DEP). To resuspend particles from the wall, a force pointing away from the wall is required, which can be DEP again. Naturally, to reverse the trapping movement, particles trapped by pDEP now have to experience nDEP and vice versa. To alternate the direction of the DEP force vector either the mediums properties (e. g., electrical conductivity or permittivity) or the electric field's frequency needs to be changed.

In this study, frequency of the applied sinusoidal voltage was modulated using a triangle-shaped function. This allows to change the frequency of the electric field constantly between two values in a controllable time. Other modulation functions may also be suitable for achieving a separation. For evaluating the resolution R_S can be calculated,[19]

$$R_s = \frac{\Delta t}{\frac{1}{2}(w_1 + w_2)}, \tag{6}$$

with Δt as time that the maximum values (I_{max}) of two peaks separates and w_x for width of the two residence time distributions. The width is defined as the distance in time between the half maximum values (FWHM).

2.1. Frequency Modulation

Due to their surface conductance, PS particles show pDEP at low frequencies and nDEP at high frequencies. Assuming a constant surface conductance (usally assumed as 1 nS [25–27]) and medium conductivity (1.2 µS cm^{-1}), the cross-over frequency from negative to positive DEP (Re(CM)=0 in Equation 3) depends only on particle size. The frequency-dependent polarizability of the particles forms the fundamental of this separation technique and can be used by varying the frequency over time periodically, as shown in Figure 1. These periodical changes from pDEP to nDEP generate multiple trapping and release cycles. The separation technique also can be used for other particle types that show frequency dependent polarizability.

Larger PS particles show pDEP in a smaller frequency bandwith and consequently, when varying the frequency as shown, for a shorter duration. Since the nDEP force is pushing the particles away from the electrodes (high field regions) it decreases with the distance covered orthogonally to the flow direction. Looking at the mobility over time, it is likely that particles with a larger diameter will cover a greater distance perpendicular to the flow direction within one cycle than smaller ones. Of course, this is only valid for channels with a sufficient height and particles with an adequate amount of pDEP. Larger particles should be eluted earlier since the carrier flow got more time to transport these particles a greater distance per cycle (Figure 2 c-f).

Preprints (www.preprints.org) | NOT PEER-REVIEWED | Posted: 3 December 2019 doi:10.20944/preprints201912.0023.v1

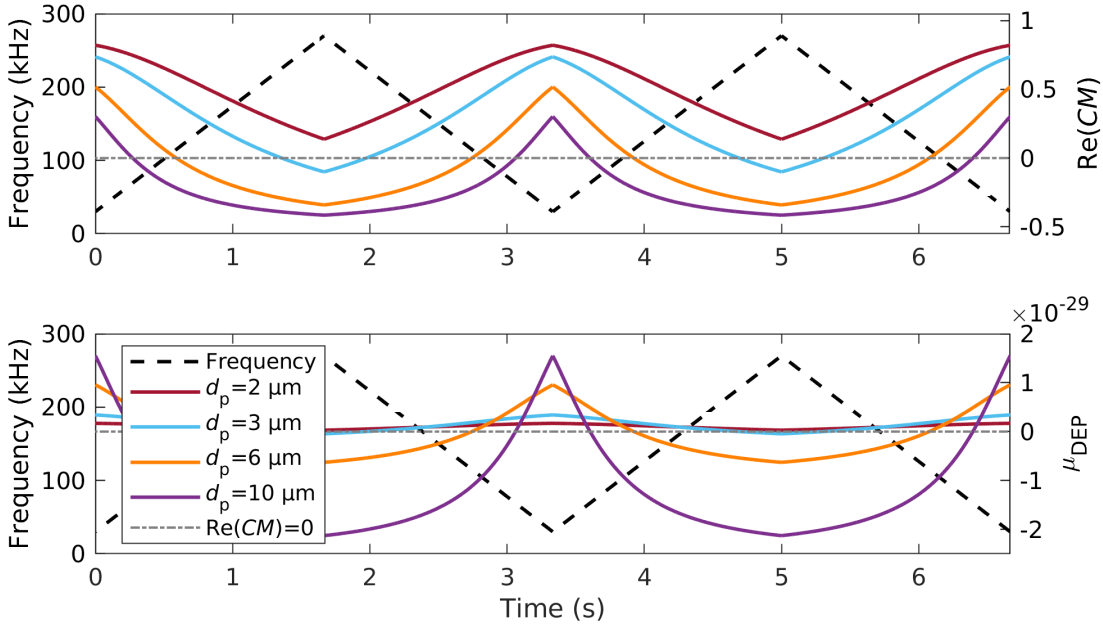

Figure 1. Real part of the Clausius-Mossotti Re(*CM*) factor (top) and dielectrophoretic mobility μ_{DEP} (bottom) of three different polystyrene particles over time for two full cycles (right ordinate axis of diagram). The modulated frequency is shown as well (left ordinate axis). Particles suspended in DI water with $\sigma_{\mathrm{m}} = 1.2\,\mu\mathrm{S\,cm^{-1}}$, $K_{\mathrm{S}} = 1\,\mathrm{nS}$ and $\varepsilon_{\mathrm{m}} = 78.5$, calculated with eqns. 3 and 4

2.2. Device Fabrication

The microfluidic device consist of two main parts. The column is formed by a 2 mm wide meandering PDMS channel (height 80 µm, length 17 cm) which provides walls and the top of the channel (Figure 2 b). The bottom is formed by the electric field generating electrode chip. Both parts were bonded using an intermediate layer as described later. The PDMS channel were produced using a SU8 master mold (soft lithography). The interdigitated electrodes (electode arm width and gap width 100 µm) were fabricated using standard cleanroom techniques. Full details of the fabrication method could be found in the SI.

The electrode-covered glass slide was bonded to the PDMS channel using liquid PDMS (10:3, base:curing agent). PDMS was selected as intermediate layer, because of its well-known spinning curves, low toxic potential and easy accessibility [28–30]. The mixed PDMS then was spin coated at 6000 rpm for 330 s on the electrodes. Using this parameters a thickness of the uncured PDMS layer should be below 3 µm [29]. Subsequently, the cleaned PDMS channel was manually aligned over the electrodes and placed onto them. The bonding was finalized by curing the intermediate layer at 80 °C for an additional two hours. The PDMS does not only allow to bond the electrodes to the channel, which proved to be unsuccessful in our lab using corona bonding, it also reduces the adhesion of the particles to the electrodes[31].

2.3. Experimental setup

Two syringe pumps are connected to a manually actuated 4-way valve (IDEX H&S V-101D). One syringe pump (kdScientific KDS-100-CE) controls the volume flow of the carrier fluid, the other pump (kdScientific LEGATO 270) provides the flow of the particle suspension (both $5\,\mathrm{mL\,h^{-1}}$). In normal position, the carrier flow is connected to the inlet of the separation column. To initiate the experiment, the valve is manually turned to allow a 2 second pulse of particle suspension to flow into the separator. The injection in all experiments happened at $t = 10\,\mathrm{s}$. The carrier fluid is pure water containing 0.02 vol % Tween20 (Sigma-Aldrich) to reduce particle wall interactions, 0.003 vol %

Preprints (www.preprints.org) | NOT PEER-REVIEWED | Posted: 3 December 2019 doi:10.20944/preprints201912.0023.v1

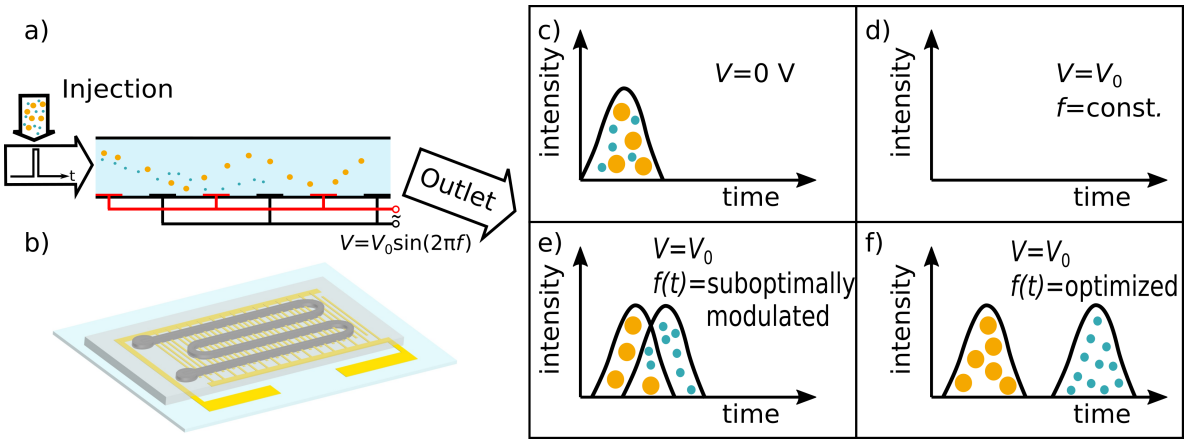

Figure 2. a) Sketch of the DPC separation experiments. b) Sketch of the DPC separation column. Meandering PDMS microchannel sealed by interdigitated electrodes on a glass chip. c-f) Different possible outlet concentrations for DPC. Without voltage, no retardation of the particles occurs and both fractions elute at the same time. (c). When the frequency is fixed, the particles are trapped in the column due to DEP and will not exit the channel. (d). If the frequency is modulated, a chromatographic separation occurs (e), which can be optimized by changing the frequencies and voltage (f).

0.01 mol L^{-1} potassium hydroxide in deionized water to adjust pH and potassium chloride to adjust the electrical conductivity to the desired value (1.2 µS cm^{-1}). The particles were suspended in the same suspension as the carrier flow, but without adding potassium chloride.

Monodisperse fluorescent polystyrene particles (Fluoresbrite, Polysciences Europe GmbH, Germany) in different sizes and colours (2 µm polychromatic red, 3 µm yellow-green and 6 µm polychromatic red, plain particles) were mixed and diluted in the described solution.

The inlet of the channel is connected to the manually actuated 4-way valve via a capillary (I.D. 100 µm) with a length of about 17 mm. To allow a controlled injection of the particles, the internal volume of the connection from valve to channel inlet should be kept as small as possible. The chosen (short and with small diameter) inlet capillary resulted in a volume of 135 nL, resulting in an average residence time of less than 100 ms in this capillary.

The electrodes were connected to a voltage amplifier (TREK PZD2000A) controlled by a signal generator (RIGOL DG4062). The signal generator provides the functionality of frequency modulation inherently. The amplifier's output signal was monitored using an oscilloscope (RIGOL DS2072A). The amplification factor of the amplifier is not constant, but decreases with increasing frequency. The output decreases by 4.3 % per 10 kHz, which results in exponential decay in the applied voltage. All stated voltages are measured at 30 kHz. This circumstance may be overcome by using a different amplifier in future experiments.

The fluorescence of the particles allows to distinguish between different particles easily by their fluorescence. To observe the particles an inverted microscope (Nikon TS2R-FL) was used. For observation a DAPI/FITC/TRITC (excitation: 387/478/555 nm, emission: 433/517/613 nm) triple bandpass was selected, which allows observing at least three different types of particles at once. However, only two particle colours could be observed simultaneously, since the current optics inhibit the DAPI excitation. Videos of the fluorescence were recorded at the outlet of the channel using a color CMOS camera (GS3-U3-51S5C-C, FLIR Integrated Imaging Solutions, Inc., Canada) which were further processed using MATLAB (see Supporting Documents for further information). In MATLAB, the frames were segmented, resulting in different pictures for each particle and background. Finally, the intensity of each picture were counted and plotted over time.

Preprints (www.preprints.org) | NOT PEER-REVIEWED | Posted: 3 December 2019 doi:10.20944/preprints201912.0023.v1

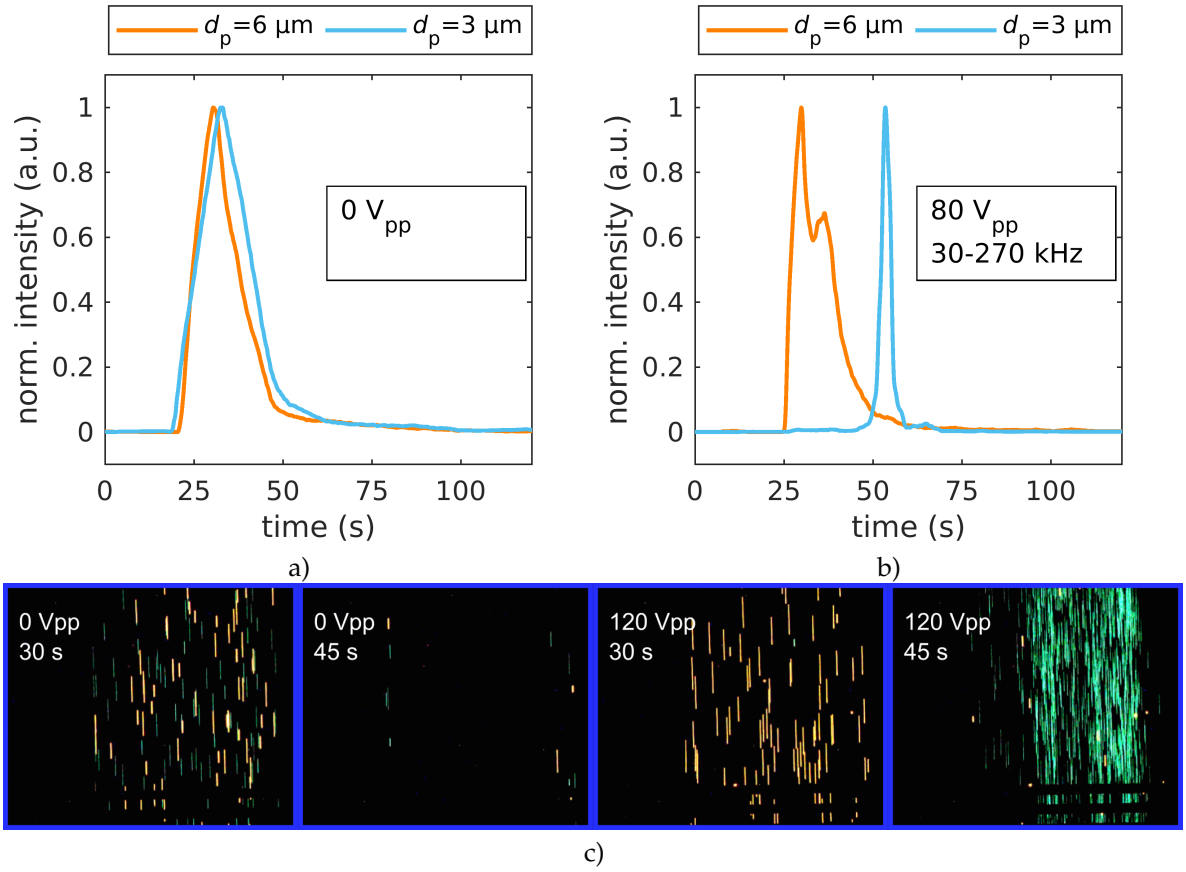

Figure 3. Fluorescence intensity over time of 3 µm and 6 µm fluorescent polystyrene particles. a) no voltage applied; $R_s = 0.17 \pm 0.06$ ($N = 4$). b) 80 V_{pp} at 30 kHz–270 kHz with a modulation frequency of 300 mHz; $R_s = 3.60 \pm 0.31$ ($N = 4$). c) Single frames of different times of 3 µm (yellow-green) and 6 µm (orange/red) fluorescent polystyrene particles (brightness and contrast are adjusted for better visibility).

3. Results and discussion

To prove the principle we separated polystyrene particles with respect to size. Microparticles with a diameter of 3 µm and 6 µm were separated by DPC (Figure 3). Without electric field, both particles sizes show typical retention time distributions for particles in a laminar flow and no separation could be observed (Figure 3 a). A chromatographic separation could be achieved for the investigated voltages of 60 V_{pp}, 80 V_{pp}, 100 V_{pp} and 120 V_{pp} (see Supporting Documents for the full data set). To achieve separation the set voltages was applied while the frequency was varied between 30 kHz–270 kHz in 3.33 s (full cycle length, 300 mHz). In this frequency range the used particles show both nDEP and pDEP in different ratios. The best resolution could be achieved for a voltage of 80 V_{pp} resulting in an average resolution of $R_s = 3.60 \pm 0.31$ (number of experiments $N = 4$) (Figure 3 b).

As expected, the 6 µm particles elute earlier than the smaller particles, which show a substantial delay with respect to measurements without electric field. Interestingly, the peak size of the 3 µm particles decreases significantly, which suggests that their retention time is dominated by DEP and not by their initial height in the channel. In contrast, the peak size and position of the 6 µm stays almost the same, which is due to a balanced nDEP/pDEP ratio presumably, whereas the smaller particles show pDEP for a wider frequency range. A balanced nDEP/pDEP leads to no net movement orthogonal to the fluid flow direction over one cycle. Consequently, at low to moderate voltages, particles are only slightly retarded in the channel caused by moving along the different streamlines of the parabolic

Preprints (www.preprints.org) | NOT PEER-REVIEWED | Posted: 3 December 2019 doi:10.20944/preprints201912.0023.v1

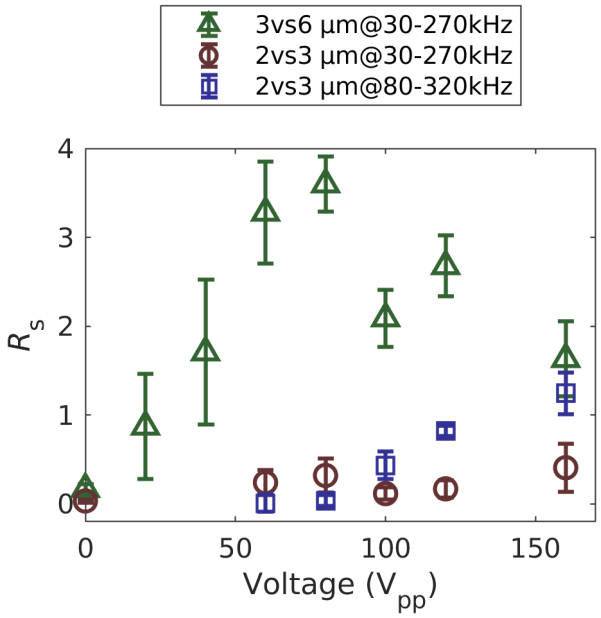

Figure 4. Resolution R_s of DPC over applied voltage for different particle suspensions and frequencies.

flow profile. At higher voltages, particles move far enough for them to hit either the electrode array, or channel ceiling, causing trapping and considerable retardation.

To investigate the effect of the voltage onto the resolution of the separation process further, particles with diameters of 2 µm and 3 µm were selected. Since the mobility of both particles are closer to each other the separation is more ambitious. Using the same set of parameters as before, we could again observe a voltage dependence (see Figure 4 and also the Supporting Documents for intensity profiles as a function of time). In contrast to the 3 vs. 6 µm experiments, there is almost no separation below 80 V_{pp}. This is because μ_{DEP} for both particle types are low and very close to each other. However, with increasing voltage the peaks begin to differ and the differences in their mobility become more visible.

The separation of the 2 and 3 µm particles could be further improved, concerning peak width and peak distance, by changing the frequency between which was varied. Applying an offset of 50 kHz (now: 80 kHz-320 kHz) the retention times of each particle type become more homogeneous (FWHM decreases) and distance between the peaks increases (Figure 4). Interestingly, the resolution is similar for both sets of frequencies for all voltages except for 160 V_{pp}, but the retention times are significantly different. At 120 V_{pp}, where the highest resolution using 30 kHz–270 kHz was achieved, the particles elute almost 15 s later than when using 80 kHz–320 kHz at the same voltage (2 µm: 55.22 s $\pm$ 6.94 s vs. 40.73 s $\pm$ 0.75 s, 3 µm: 49.06 s $\pm$ 5.32 s vs. 36.86 s $\pm$ 0.84 s, both N=4). We assume that, due to the higher frequencies, an increased negative dielectrophoretic movement pushes the particles away from the electrodes and thus towards higher fluid velocities. Although the residence time of the particles is much shorter when applying 80 kHz-320 kHz, the resolution stays the same at 120 V_{pp} and increases even further to $R_s = 1.25 \pm 0.23$, $(N = 4)$, when the voltages is set to 160 V_{pp}, which does not occur using the lower frequency set. This shows the potential of adjusting the stationary phase (electric field) for separation, which needs to be investigated further to develop design rules. Nevertheless, again, the particles larger in diameter elute earlier and in contrast to the 6 µm particles, both particles show an increase in retention time with respect to the measurements without electric field and therefore without superimposed dielectrophoretic movement.

The resolution of the separation (Figure 4) increases with increasing voltage in the conducted experiments until to a certain voltage is reached. For separating 3 and 6 µm this voltage is reached at 80 V_{pp}, afterwards the resolution decreases. This is mainly because the retention time of bigger

Preprints (www.preprints.org) | NOT PEER-REVIEWED | Posted: 3 December 2019 doi:10.20944/preprints201912.0023.v1

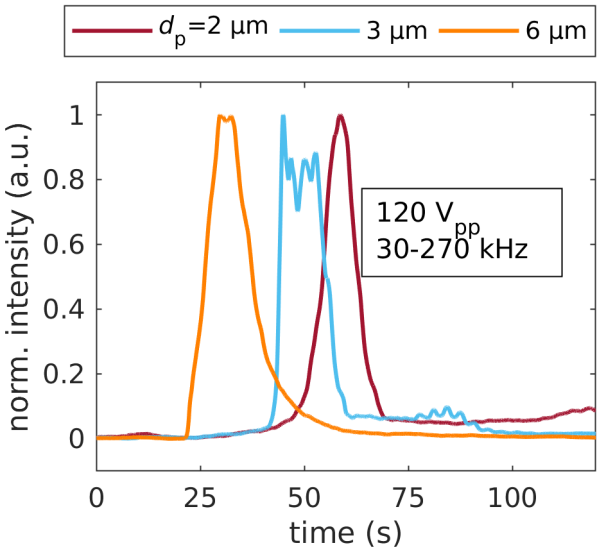

Figure 5. Overlay of the averaged fluorescence intensity of the experiments from separating 2 µm from 3 µm and 3 µm from 6 µm. All experiments were performed at 120 V_{pp} and at a frequency of 30 kHz - 270 kHz. The 3 µm intensity is averaged from both separations (N=6). For 2 µm and 6 µm retention time $N = 3$.

particles increase with voltage (80 V_{pp}: 27.92 s ± 1.74 s to 160 V_{pp}: 40.8 s ± 3.33 s, both $N = 4$), whereas the time of the maximum fluorescence intensity for the smaller particles stays almost the same. The increase of the retention time of the bigger particles may be due to decreasing travel times orthogonal to the fluid flow because at this high field strength the particle reach the electrodes at low frequencies and are retarded as a consequence.

The resolution increases with increasing voltage for the 2 and 3 µm mixtures also. In contrast to the case involving the 6 µm particles, no significant decrease occurs at the maximum applied voltage investigated, which suggests an increase in voltage may lead to a further increased resolution.

Since the dielectrophoretic velocity depends quadratically on the particle's radius and the applied electric field, the size and voltage dependency is not surprising. Due to this, smaller particles accelerate less due to DEP. Additionally, the cross-over frequency at which the force switches from pDEP to nDEP is higher, i.e. small particles experience pDEP for a longer duration per cycle. Consequently, small particles, once they come close to the interdigitated electrodes, remain there and thus in regions of low fluid velocity. The latter point should become more important as the residence time in the separation column increases (i.e., at longer column length).

Finally, an overlay of the averaged experiments from separating 2 µm from 3 µm and 3 µm from 6 µm at 120 V_{pp} and a frequency 30 kHz–270 kHz indicates that a separation of all three different particle types in one run should be possible (Figure 5). With the current hardware it is not possible to observe all three different kinds of particles at the same time. However, the current dataset suggests that this approximation is legitimate since the retention times of the 3 µm particles are similar at this voltage (retention times of the 3 µm particles: $t_{peak} = 49.06\,s \pm 5.32\,s$ vs. 2 µm and 47.64 s ± 4.73 s vs. 6 µm).

Although the frequency bandwidth (30 kHz–270 kHz), as the experiments suggest, is not optimal for separation of 2 and 3 µm particles, a separation of 2 µm, 3 µm, 6 µm seems to be possible.

Despite the fact that the parameters where chosen by evaluating the mobility of the particles over the frequency and only model particles where evaluated, the technique can become a tool for chromatographic separation of arbitrary particles that show a frequency-dependent polarizability. One major advantage of this technique is, that the columns' parameter are adjustable without actually

 doi:10.20944/preprints201912.0023.v1

changing the column itself. As shown the electric field strength and the frequency bandwidth have an impact on the retention times and the peak width.

4. Conclusion

In the experiments two binary mixtures of suspended particles could be separated using dielectrophoretic particle chromatography with a modulated electric field frequency. Additionally, the potential for separating three particle types was illustrated, by superimposing two binary particle separations. We believe that an increasing column length should lead to even better separation. In addition to this, without using a manually opened injection valve standard deviations should decrease significantly since the timing of a machine is much more accurate. The influence of other parameters such as the modulating frequency, the medium's electrical conductivity, the linearity of amplification and the carrier fluids' volume flow are complex and not cleared in detail and a comprehensive study regarding their impact is under way. Nevertheless, the effect of the applied voltage was discussed and increasing the resolution by changing the frequency band was shown. In the proposed chromatography column no single trap and release mechanism was used to achieve a chromatographic separation, but the particles show different interactions with the permanently present and adjustable stationary phase. Albeit only model particles were investigated in this study, the presented method allows to chromatographically separate arbitrary particles with frequency-dependent polarizability. We believe that the presented technique can potentially separate particle mixtures that are traditionally difficult to separate, for instance, cell separation in liquid biopsy or the recovery of precious materials from waste streams.

Author Contributions: J. Giesler, G. Pesch, M. Baune, and J. Thöming conceived the experiments. J. Giesler conducted the experiments. M. Schmidt fabricated the electrodes and SU8 master and contributed their layout. J. Giesler, G. Pesch, L. Weirauch, M. Baune, and J. Thöming analysed the results. G. Pesch and M. Baune supervised the project. J. Giesler wrote the manuscript with input from all other authors.

Funding: This work was funded by the German Research Foundation (DFG) within the priority program, "MehrDimPart - Highly specific and multidimensional fractionation of fine particle systems with technical relevance" (SPP2045, grant number BA 1893/2-1).

Acknowledgments: The authors thank Jonathan Kottmeier (IMT, TU Braunschweig) for the help in manufacturing components of the separation column and Fei Du (CVT, Universität Bremen) for fruitful discussions.

Conflicts of Interest: The authors declare no conflict of interest.

Abbreviations

The following abbreviations are used in this manuscript:

AC	alternating current
CM	Clausius-Mossotti-factor
DEP	dielectrophoresis
DPC	dielectrophoretic particle chromatography
FWHM	full width at half maximum
nDEP	negative dielectrophoresis
pDEP	positive dielectrophoresis
PDMS	polydimethylsiloxane

References

1. Vahey, M.D.; Voldman, J. An equilibrium method for continuous-flow cell sorting using dielectrophoresis. *Analytical Chemistry* **2008**, *80*, 3135–3143. doi:10.1021/ac7020568.
2. Moon, H.S.; Kwon, K.; Kim, S.I.; Han, H.; Sohn, J.; Lee, S.; Jung, H.I. Continuous separation of breast cancer cells from blood samples using multi-orifice flow fractionation (MOFF) and dielectrophoresis (DEP). *Lab on a Chip* **2011**, *11*, 1118. doi:10.1039/c0lc00345j.

3. Henslee, E.A.; Sano, M.B.; Rojas, A.D.; Schmelz, E.M.; Davalos, R.V. Selective concentration of human cancer cells using contactless dielectrophoresis. *Electrophoresis* **2011**, *32*, 2523–2529. doi:10.1002/elps.201100081.
4. Wang, X.B.; Yang, J.; Huang, Y.; Vykoukal, J.; Becker, F.F.; Gascoyne, P.R.C. Cell separation by dielectrophoretic field-flow-fractionation. *Analytical Chemistry* **2000**, *72*, 832–839. doi:10.1021/ac990922o.
5. Washizu, M.; Suzuki, S.; Kurosawa, O.; Nishizaka, T.; Shinohara, T. Molecular dielectrophoresis of bio-polymers. *Conference Record - IAS Annual Meeting (IEEE Industry Applications Society)* **1992**, *1992-Janua*, 1446–1452. doi:10.1109/IAS.1992.244397.
6. Spengler, T.; Ploog, M.; Schröter, M. Integrated planning of acquisition, disassembly and bulk recycling: A case study on electronic scrap recovery. *OR Spectrum* **2003**, *25*, 413–442.
7. Du, F.; Baune, M.; Kück, A.; Thöming, J. Dielectrophoretic gold particle separation. *Separation Science and Technology* **2008**, *43*, 3842–3855. doi:10.1080/01496390802365779.
8. Williams, S.K.R.; Runyon, J.R.; Ashames, A.A. Field-flow fractionation: Addressing the nano challenge. *Analytical Chemistry* **2011**, *83*, 634–642. doi:10.1021/ac101759z.
9. Hanauer, M.; Pierrat, S.; Zins, I.; Lotz, A.; Sönnichsen, C. Separation of nanoparticles by gel electrophoresis according to size and shape. *Nano Letters* **2007**, *7*, 2881–2885. doi:10.1021/nl071615y.
10. Wei, G.T. Shape separation of nanometer gold particles by size-exclusion chromatography. *Analytical Chemistry* **1999**, *71*, 2085–2091. doi:10.1021/ac990044u.
11. Pesch, G.R.; Lorenz, M.; Sachdev, S.; Salameh, S.; Du, F.; Baune, M.; Boukany, P.E.; Thöming, J. Bridging the scales in high-throughput dielectrophoretic (bio-)particle separation in porous media. *Scientific Reports* **2018**, *8*, 1–12. doi:10.1038/s41598-018-28735-w.
12. Suehiro, J.; Zhou, G.; Imamura, M.; Hara, M. Dielectrophoretic filter for separation and recovery of biological cells in water. *IEEE Transactions on Industry Applications* **2003**, *39*, 1514–1521. doi:10.1109/TIA.2003.816535.
13. Modarres, P.; Tabrizian, M. Frequency hopping dielectrophoresis as a new approach for microscale particle and cell enrichment. *Sensors and Actuators, B: Chemical* **2019**, *286*, 493–500. doi:10.1016/j.snb.2019.01.157.
14. Wang, Y.; Du, F.; Pesch, G.R.; Köser, J.; Baune, M.; Thöming, J. Microparticle trajectories in a high-throughput channel for contact-free fractionation by dielectrophoresis. *Chemical Engineering Science* **2016**, *153*, 34–44. doi:10.1016/j.ces.2016.07.020.
15. Sano, H.; Kabata, H.; Kurosawa, O.; Washizu, M. Dielectrophoretic chromatography with cross-flow injection. *Technical Digest. MEMS 2002 IEEE International Conference. Fifteenth IEEE International Conference on Micro Electro Mechanical Systems (Cat. No.02CH37266)* **2002**, pp. 2–5. doi:10.1109/MEMSYS.2002.984043.
16. Kikkeri, K.; Ngu, B.; Agah, M.; Engineering, C.; Tech, V. Submicron Dielectrophoretic Chromatography **2018**. pp. 1177–1180.
17. Umezawa, Y.; Kobayashi, O.; Kanai, S.; Hakoda, M. Development of Particle Packed Bed Type Chromatography Using Dielectrophoresis. *Key Engineering Materials* **2013**, *534*, 88–92. doi:10.4028/www.scientific.net/KEM.534.88.
18. Hakoda, M.; Otaki, T. Analytical Characteristic of Chromatography Device Using Dielectrophoresis Phenomenon. *Key Engineering Materials* **2012**, *497*, 87–92. doi:10.4028/www.scientific.net/KEM.497.87.
19. Aldaeus, F.; Lin, Y.; Amberg, G.; Roeraade, J. Multi-step dielectrophoresis for separation of particles. *Journal of Chromatography A* **2006**, *1131*, 261–266. doi:10.1016/j.chroma.2006.07.022.
20. Green, N.G.; Hughes, M.P.; Monaghan, W.; Morgan, H. Large area multilayered electrode arrays for dielectrophoretic fractionation, 1997. doi:10.1016/S0167-9317(96)00122-0.
21. Cheng, I.F.; Froude, V.E.; Zhu, Y.; Chang, H.C.; Chang, H.C. A continuous high-throughput bioparticle sorter based on 3D traveling-wave dielectrophoresis. *Lab on a Chip* **2009**, *9*, 3193–3201. doi:10.1039/b910587e.
22. Sun, T.; Morgan, H.; Green, N.G. Analytical solutions of ac electrokinetics in interdigitated electrode arrays: Electric field, dielectrophoretic and traveling-wave dielectrophoretic forces. *Physical Review E - Statistical, Nonlinear, and Soft Matter Physics* **2007**, *76*, 1–18. doi:10.1103/PhysRevE.76.046610.
23. García-Sánchez, P.; Ramos, A.; González, A.; Green, N.G.; Morgan, H. Flow reversal in traveling-wave electrokinetics: An analysis of forces due to ionic concentration gradients. *Langmuir* **2009**, *25*, 4988–4997. doi:10.1021/la803651e.

24. Hughes, M.P. Fifty years of dielectrophoretic cell separation technology. *Biomicrofluidics* **2016**, *10*. doi:10.1063/1.4954841.
25. Pethig, R. Dielectrophoresis: Status of the theory, technology, and applications. *Biomicrofluidics* **2010**, *4*. doi:10.1063/1.3456626.
26. Ermolina, I.; Morgan, H. The electrokinetic properties of latex particles: Comparison of electrophoresis and dielectrophoresis. *Journal of Colloid and Interface Science* **2005**, *285*, 419–428. doi:10.1016/j.jcis.2004.11.003.
27. Arnold, W.M.; Schwan, H.P.; Zimmermann, U. Surface conductance and other properties of latex particles measured by electrorotation. *Journal of Physical Chemistry* **1987**, *91*, 5093–5098. doi:10.1021/j100303a043.
28. Satyanarayana, S.; Karnik, R.N.; Majumdar, A. Stamp-and-stick room-temperature bonding technique for microdevices. *Journal of Microelectromechanical Systems* **2005**, *14*, 392–399. doi:10.1109/JMEMS.2004.839334.
29. Gajasinghe, R.W.; Senveli, S.U.; Rawal, S.; Williams, A.; Zheng, A.; Datar, R.H.; Cote, R.J.; Tigli, O. Experimental study of PDMS bonding to various substrates for monolithic microfluidic applications. *Journal of Micromechanics and Microengineering* **2014**, *24*. doi:10.1088/0960-1317/24/7/075010.
30. Koschwanez, J.H.; Carlson, R.H.; Meldrum, D.R. Thin PDMS films using long spin times or tert-butyl alcohol as a solvent. *PLoS ONE* **2009**, *4*, 2–6. doi:10.1371/journal.pone.0004572.
31. Wang, X.B.; Vykoukal, J.; Becker, F.F.; Gascoyne, P.R. Separation of polystyrene microbeads using dielectrophoretic/gravitational field-flow-fractionation. *Biophysical Journal* **1998**, *74*, 2689–2701. doi:10.1016/S0006-3495(98)77975-5.